

Self-supervised Extraction of Human Motion Structures via Frame-wise Discrete Features

Tetsuya Abe^{1,2}, Ryusuke Sagawa^{1,2*}, Ko Ayusawa^{1,2}
and Wataru Takano³

^{1*}Tokyo University of Agriculture and Technology, Koganei,
Tokyo, Japan.

^{2*}National Institute of Advanced Industrial Science and
Technology, Tsukuba, Ibaraki, Japan.

³Osaka University, Toyonaka, Osaka, Japan.

*Corresponding author(s). E-mail(s): ryusuke.sagawa@aist.go.jp;

Contributing authors: s211948v@st.go.tuat.ac.jp;

k.ayusawa@aist.go.jp; takano@sigmath.es.osaka-u.ac.jp;

Abstract

The present paper proposes an encoder-decoder model for extracting the structures of human motions represented by frame-wise discrete features in a self-supervised manner. In the proposed method, features are extracted as codes in a motion codebook without the use of human knowledge, and the relationship between these codes can be visualized on a graph. Since the codes are expected to be temporally sparse compared to the captured frame rate and can be shared by multiple sequences, the proposed network model also addresses the need for training constraints. Specifically, the model consists of self-attention layers and a vector clustering block. The attention layers contribute to finding sparse keyframes and discrete features as motion codes, which are then extracted by vector clustering. The constraints are realized as training losses so that the same motion codes can be as contiguous as possible and can be shared by multiple sequences. In addition, we propose the use of causal self-attention as a method by which to calculate attention for long sequences consisting of numerous frames. In our experiments, the sparse structures of motion codes were used to compile a graph that facilitates visualization of the relationship between the codes and the differences between sequences. We then evaluated the effectiveness of the extracted motion codes by applying them to

multiple recognition tasks and found that performance levels comparable to task-optimized methods could be achieved by linear probing.

Keywords: Human motion analysis, Discrete latent space, Self-supervised learning, Visualization, Self-attention, VQ-VAE

1 Introduction

Improved recognition of human behaviors will provide important progress toward realizing advanced technologies, such as human-robot interactions. However, one of the difficulties with action recognition can be traced to the continuity of human motions because even just a few seconds of motion will contain several smoothly connected actions. In order to minimize the effects of this complexity, most existing human action recognition methods use motion data with annotations added for specific motion segments. In efforts aimed at learning segmented motion data, recent research has successfully extracted motion features that are useful for action recognition [1–3]. These methods, which assume that the given motions have the same level of granularity, seek to identify recurring or similar motion sequence patterns in latent space. The extracted features are usually convoluted with the whole-motion sequence. However, the effectiveness of such feature representations strongly depends on the granularity of the motion annotations that are applied during the training phase. For example, when a sequence of walking data is given, the entire sequence is converted to a feature that can represent “walking”, but its meaning cannot be subdivided in latent space into “one step with the left foot” or “one step with the right foot”. Since this fixed-granularity problem is found in the human motion features of all of these methods, their applicability to multiple applications is limited to generalizations that require different levels of representation granularity.

Human motions consist of multiple stages, each of which is influenced by the characteristics of the individual human or the contexts of specific motions. Therefore, it is necessary to extract representations of multiple spatial and temporal components in order to effectively recognize these motions. Taken further, if it were possible to extract the unique representations of a specific individual, this would be very useful for understanding the characteristics of his or her human motions. For example, this could help to explain the differences in the motions between beginners and experts. However, since each individual possesses unique representations that are not shared among others, the actions of one person are not expected to completely match the shared knowledge of others in a manner similar to natural language. Therefore, first among the three primary issues to be resolved is finding a way to extract a unique representation without using preexisting knowledge.

Typically, human motions are expressed as multi-dimensional continuous quantities, such as joint angles at each sampling moment. However, when we

consider the case of generating a new motion, specifying all joint angles at each moment is difficult. Therefore, in order to make it feasible to specify such values, representations which are a finite number of components or parameters are required. This is the second representation issue that must be addressed.

Since the components that make up a motion have temporal relationships with each other, the recognition of the motion is equivalent to identifying those relationships. In addition, since any human motion will have a relationship with motions that took place several seconds or more previously, the temporal receptive field for the recognition should be wider than the dependency. Furthermore, since it is necessary for the recognition of human motions, the receptive field should be wider than several hundred frames. Therefore, the third issue is determining a recognition method that can be used with a wide receptive field.

With the above motivations in mind, our goal is to extract identifiable features that can be used to represent human motions without using preexisting knowledge (annotated motion data). The contributions of the present study are as follows. We show how an intermediate representation of human motion can be generated in latent space based on an encoder-decoder model without using preexisting knowledge (annotated motion data). The representation consists of a finite number of components that are obtained by discretizing the latent space, and the proposed method realizes a wide temporal receptive field by using an attention-based network to extract relationships in a long sequence.

2 Related work

The process of understanding human behavior is typically categorized into several tasks, such as action recognition and action segmentation. Action recognition is defined as the task of finding areas of correspondence between input data and action labels. In this task, the system basically identifies answers with actions that match the input data. Hence, in supervised approaches, action labels are assigned, and the target actions to be detected are fixed. As examples, previously methods proposed [4–6] determine actions based on supervised learning directly from video footage used as input data.

Another approach by which to determine actions is to use skeletal information acquired by detecting human poses or by using a motion capture system [7–9]. Some methods based on skeletal information [10–15] define the problem as a translation between motion and language. However, since the cost of obtaining input data, such as videos with action labels, is high, unsupervised approaches, such as pre-training, have been used to learn representations from video footage [16]. In these methods, latent spaces are learned from skeletal information based on self-supervised approaches [1, 17].

Action segmentation is the task of segmenting a temporal sequence of input data into multiple actions. A number of methods [18–20] determine multiple action types and their boundaries in examined video frames based on supervised learning. Unsupervised approaches to action segmentation that work by

using clustering to find the same actions [21–23] and aligning phases [24] have also been proposed.

Separately, since numerous actions are said to have hierarchical structures, which means multi-level action labels can be defined, other previous methods based on supervised learning [25–29] have proposed the use of fine-grained action labels to explain coarse-level actions. For example, a method proposed in a previous study [30] learns the latent space of sub-actions by means of an unsupervised approach based on clustering. Using skeletal information to learn the representations of human motion based on unsupervised learning is a method that can also be used for other tasks. For example, when examining video footage, the joint angles of the next frame have been predicted using previous frame data [31–34].

One of the major approaches used to explain human actions is to find relationships between the motions and the words of natural languages. Since words are common knowledge, the parts of an action can be readily understood by users. Hence, various methods of facilitating mutual translations between motions and language have been studied. These approaches can achieve a useful intermediate representation of motion by finding the relationship between a motion and a language. In one example, a motion language model encoded by a hidden Markov model (HMM) was used as an intermediate representation to express the relationships between motions and language [11].

Separately, a context vector encoded by a recurrent neural network (RNN) was used to provide an intermediate representation of motion [12], which allowed human motions to be generated from the input text by learning the intermediate representation as the output of an RNN based on a generative adversarial network (GAN) in [13], while an autoencoder for motion and language that calculates two latent vectors has also been proposed [14]. In the latter method, the difference between the latent vectors is minimized in training and then used as the intermediate representation. Joint embedding of the latent vectors has been used for an autoencoder [15], which reproduces the motion from the joint vector, and the latent vector of the language encoder is only used in inference time. However, in all of these approaches, the intermediate representations of the motion are supervised by the annotations using language labels, which means representing unique characteristics that cannot be expressed by language is difficult.

Furthermore, while these supervised or self-supervised methods with annotated (segmented) motion data can extract the motion features for action recognition, the latent space obtained in this manner is mediated by human knowledge that segments the motion data, which means that these methods require motion data with an appropriate level of granularity. In order to avoid this problem, we propose a method that can extract feature representations without preexisting human knowledge (segmented motion data with annotation label). More specifically, the proposed method is based on a variational autoencoder that generates a discrete latent space, such as a vector quantized-variational autoencoder (VQ-VAE) [35] or a dynamical variational

autoencoder (dVAE) [36]. Temporal relationships between frames are found based on self-attention, as proposed in the Transformer [37]. The great benefit of discrete representation is its ability to find the discontinuous points of motion data and thus help in detecting actions in non-segmented motion data.

3 Proposed method

The proposed method extracts the discrete motion feature of each frame in a long sequence. Once extracted, the motion feature is regarded as a motion code in a motion codebook, which is a set of components used to explain various motions. The purpose of such frame-wise feature extraction is to obtain motion codes independently of existing knowledge. However, since the proposed method does not use segmented motion data, the limited receptive field of a convolutional network is unsuitable. Accordingly, the proposed method uses a self-attention architecture, and a vector-quantized framework [35] to find discrete representations among motion data by considering temporal relationships over a wide range of frames. The temporal dependency of human motions is unknown but is considered to be more than several seconds. For example, the receptive field of the network used along the time axis should be several hundred frames wide if the motion is captured at 100 Hz.

3.1 Encoder-decoder with discrete latent space

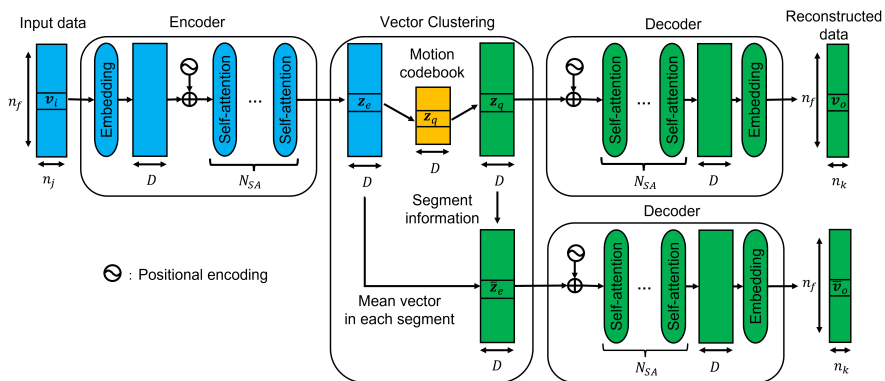


Fig. 1 Proposed model consisting of an encoder, a decoder, and vector clustering, which has two outputs: z_q and \bar{z}_e . The former is a motion code replaced from the encoder output, and the latter is the mean vector of a segment of the same motion code

The proposed method generates a discrete latent space that describes the structure of a human motion using a network consisting of an encoder and a decoder combined with a block of clustering latent vectors that are used to extract discrete motion codes. Vector clustering is realized as a quantization process that maps the encoder output to the nearest embedding vector in a

motion codebook. In the proposed study, this quantization is implemented based on VQ-VAE [35], and the encoder and decoder are realized by self-attention layers [37] in order to find relationships between frames.

The architecture of the proposed model is shown in Fig. 1. The input data of a motion consist of n_f frames of n_j -dimensional vectors at each frame, and the encoder converts the input vector \mathbf{v}_i at each frame to a feature vector \mathbf{z}_e . The vector clustering has two outputs: one output replaces \mathbf{z}_e with the vector \mathbf{z}_q , which is the nearest neighbor in the codebook based on Euclidean distance in the latent space. Note that the codebook itself consists of 512 kinds of embedding vectors \mathbf{z}_q in latent space. The other output replaces an encoded vector with the mean vector $\bar{\mathbf{z}}_e$ of each segment, which consists of consecutive frames of the same motion code \mathbf{z}_q . The difference between \mathbf{z}_q and $\bar{\mathbf{z}}_e$ is considered to be the parameter of a segment that represents variations in the same cluster. Since \mathbf{z}_q does not contain this parameter, we refer to it as the default parameter. The decoder reconstructs the outputs \mathbf{v}_o and $\bar{\mathbf{v}}_o$ using \mathbf{z}_q and $\bar{\mathbf{z}}_e$, respectively.

The outputs are framewise human motions that correspond to the input. If the input is motion, then the model is designed as an autoencoder. However, the input can also be other modalities, such as first-person video input by the subject. In the present paper, a high-dimensional video input is assumed to have already been encoded frame by frame for use as a feature vector and that the temporal relationship has already been extracted by the proposed model.

3.2 Layered causal self-attention for a long sequence

The input sequence length can be more than a thousand frames if, for example, it is captured for more than one minute at 30 frames per second (fps). Because identifying every combination of frames by self-attention due to time and memory limitations is not feasible, the attention matrix is only calculated for a portion of a sequence even if the multiple self-attention layers proposed in [37] are used. Therefore, for example, the attention is calculated for $M (< N)$ frames as the attention width, even though the sequence has a total of N frames. In this section, the use of layered causal self-attention is proposed to overcome this limitation.

In the human motion extraction task, it can be assumed that the output motion is causal only for the past input and output. However, since simply masking future frames will not decrease computational costs, the proposed approach only calculates the attention between each frame and its preceding $M - 1$ frames. The output \mathbf{z} of self-attention is calculated using the following equation:

$$\mathbf{z} = \text{softmax}\left(\frac{\mathbf{Q}\mathbf{K}^T}{\sqrt{D}}\mathbf{V}\right) \quad (1)$$

where \mathbf{Q} , \mathbf{K} , and \mathbf{V} are the query, key, and value vectors, and D is the dimension of the feature vector.

Fig. 2(a) is an input sequence and Fig. 2(b) is the attention mask for each frame. The dimensions are the batch size B , the number of value vectors, and the number of query/key vectors. The vectors are rearranged so that the attention is calculated between a single value vector and vectors of the preceding $M - 1$ frames, as shown in Fig. 2(c). The value vector is the feature of the last frame of each row in Fig. 2(c), and output \mathbf{z} is obtained with attention width M for every frame except the beginning of the sequence. If the number of attention layers is N_{SA} , then the total receptive field size is $N_{SA}M$ frames for every frame. For preceding frames that are less than M , the query and key vectors are padded by zero vectors. Since the attention is calculated for the last frame, the positional encoding is given as a position relative to the value vector frame. Therefore, the positional encoding values are the same in each column in Fig. 2(c). In the present study, the method used to calculate the position is the same as that used in the original Transformer. The output is rearranged again, as shown in Fig. 2(e), and then used as input for the feed-forward network in the same manner as proposed in the Transformer.

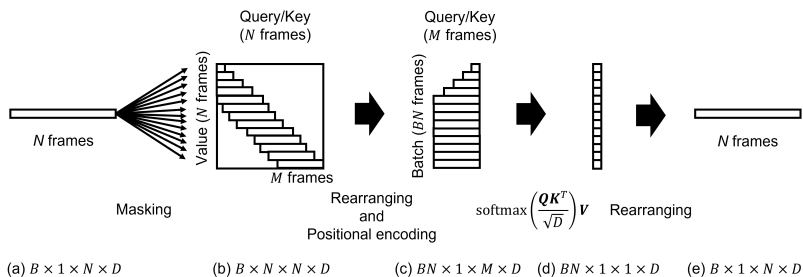


Fig. 2 Attention is calculated only for preceding frames. By rearranging the vectors, a wide receptive field is realized with a narrow attention width for each layer. The sizes indicate the number of vectors or vector dimensions: Batch \times Value \times Query/Key \times Feature

3.3 Loss for extracting motion codes shared by sequences

If the network is optimized to reconstruct the output \mathbf{v}_o without using any constraint to share motion codes, then each sequence will be reconstructed using unique codes. However, if the latent space forms a structure of human motions, a latent vector extracted by the proposed method is regarded as a motion code that is expected to be shared by multiple sequences. Hence, the following loss L is proposed to encourage motion code sharing:

$$L = \sum_k^{n_f} \alpha L_{\text{reconst}} + L_{\text{latent}} \quad (2)$$

where L_{reconst} and L_{latent} are the losses of reconstruction and latent space, respectively, for the k -th frame of a motion sequence of n_f frames, and α is a user-defined weight of the reconstruction loss, as are β and γ in equations presented later.

3.3.1 Reconstruction loss

The reconstruction loss is calculated with the parameter of each segment and the default parameter. In the proposed method, it is assumed that the default parameter of a motion code indicates temporally local motion. The loss with the constraint of local motion is defined as follows:

$$L_{\text{reconst}} = L_{\text{p}} + L_{\text{v}} \quad (3)$$

$$L_{\text{p}} = \| \mathbf{v}_{ik} - \bar{\mathbf{v}}_{ok} \|^2 \quad (4)$$

$$L_{\text{v}} = \| \dot{\mathbf{v}}_{ik} - \dot{\mathbf{v}}_{ok} \|^2 \quad (5)$$

where L_{p} is the reconstruction loss with the parameter of each segment, and L_{v} is that of a local motion. In addition, L_{p} is calculated as the difference of the output vectors, and L_{v} is calculated as the difference of the temporal derivative of these output vectors. If the output vectors refer to the position, the default parameter constraint is imposed on the velocity of the vectors.

3.3.2 Latent space loss

The second part of loss L is the latent space loss, which is defined as follows:

$$L_{\text{latent}} = L_{\text{vc}} + L_{\text{tv}} \quad (6)$$

$$L_{\text{vc}} = \| \text{sg}[\mathbf{z}_{qk}] - \mathbf{z}_{ek} \|^2 + \beta \| \mathbf{z}_{qk} - \text{sg}[\mathbf{z}_{ek}] \|^2 \quad (7)$$

$$L_{\text{tv}} = \gamma \| \dot{\mathbf{z}}_{qk} \|_1 \quad (8)$$

where L_{vc} is the loss of vector clustering, and L_{tv} is that of the temporal change of quantized latent vectors. Here, L_{vc} is based on the vector quantization [35] used to make the encoded vector \mathbf{z}_{ek} easy to quantize, and \mathbf{z}_{qk} is

an entry in the motion codebook. The function sg is the stop-gradient operator that is defined as an identity at the forward computation time and has zero derivatives. Moreover, L_{TV} is the constraint that ensures the same motion code continues for as long as possible and is realized by minimizing the total variation defined by L^1 norm.

3.3.3 Restricting motion codes

Let S be a subset of input sequences that includes all types of motion in the dataset, and let Z_q be the subset of motion codes used to encode the sequences in S . In this case, all sequences in the input dataset must be reconstructed using the subset Z_q . Since different subsets Z_{q_j} ($j = 1, \dots, J$) can be taken from the input dataset with J sequences, the loss is minimized by restricting the codebook to a subset Z_{q_j} that is randomly chosen. In the first epoch, all codes are used for encoding, and one of the subsets is used to encode each sequence after the second epoch. Restricting the set of motion codes ensures that the codes are shared.

3.4 Visualizing the structure of motion codes

The decoder generates human motion from motion codes. Therefore, the attention weight for a frame indicates the frames referenced during generation. By considering multiple layers of attention and residual connections, the weight matrix \mathbf{W} is calculated from the attention weight \mathbf{W}_i ($i = 1, \dots, N_{SA}$) of the i -th decoder attention layer as follows:

$$\mathbf{W} = (\mathbf{I} + \mathbf{W}_{N_{SA}}) \cdots (\mathbf{I} + \mathbf{W}_2)(\mathbf{I} + \mathbf{W}_1) \quad (9)$$

where \mathbf{I} is the identity matrix. Since the length N of input sequences is longer than the number of frames M for the attention layers, \mathbf{W}_i is calculated by concatenating the attention weights of partial sequences.

High-weight frames, which are important for reconstructing motion, can be considered as keyframes. We have observed that the quantized latent space defined using motion codes generates high attention weights more sparsely, as compared to the continuous latent space defined by the basic use of a variational autoencoder (VAE) [38]. Fig. 3 shows an example of the sum of attention weights for each query/key frame. These two graphs show the same part of a sequence decoded by a basic VAE model (Fig. 3(a)) and by the proposed model (Fig. 3(b)). This example is one of the sequences in the JHU-ISI gesture and skill assessment working set (JIGSAWS) [39], and the background color indicates the action labels given in the dataset. Although the distribution of the weights is dense in Fig. 3(a), the proposed model generates a sparse distribution in Fig. 3(b). Since high weights can be observed for the frames close to the label boundaries, the weights appear to have some semantic meaning.

In order to extract sparse keyframes, we propose counting the top-1 frame weight for each frame. Fig. 4(a) shows the top-1 frame weight for each value

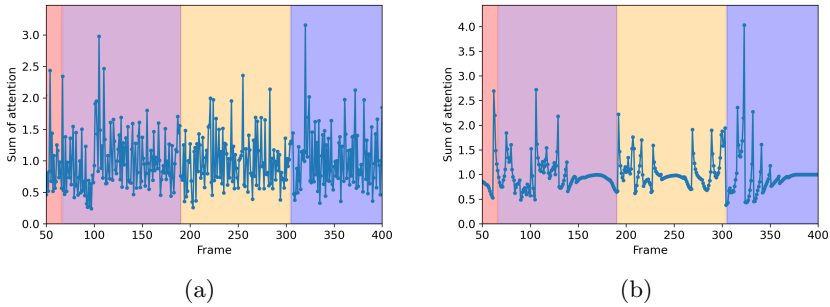


Fig. 3 Sum of attention weights for each query/keyframe: (a) basic variational autoencoder (VAE) model, (b) proposed model

vector, and Fig. 4(b) is the number of top-1 frames larger than one, which are used as keyframes. The motion code transitions assigned to the keyframes are shown in Fig. 4(c). By counting these transitions, the relationships between them can be used to form a graph, as shown in Fig. 5. The positions of the motion codes within the graph are calculated by the Fruchterman-Reingold force-directed algorithm [40] implemented in NetworkX [41]. The motion codes that correspond to three of the annotation labels are enclosed by dotted lines. The labels that occur subsequently (G2 and G3) share the motion codes, while the labels that occur at the different phases of the motion (G4) use separate motion codes.

4 Experiments

As a dataset that contains multiple components in each sequence of human motion, the JIGSAWS dataset [39], which contains video and kinematic data for robotic surgical tasks performed by operators with different skill levels, is first used in our experiments. In the present study, the suturing task, with 39 trials produced using eight subjects, is evaluated. For annotation purposes, 10 labels are used to describe actions at each frame, and the skill level (novice, intermediate, or expert) is given for each subject. The split of training and test sequences is the same as that of the setting in [42] for cross-validation.

In the kinematic data provided in JIGSAWS, six-dimensional poses for the grippers and the gripper angles of the two robot arms at each frame are used as the input/output data, which means that 14 variables are calculated for each frame. Each recorded sequence is between one and three minutes long and is captured at 30 fps at 640×480 pixels. First, the kinematic data are used as the input of the proposed method. The hyperparameters of the model in the present paper are as follows. The number of attention layers is $N_{SA} = 6$ for both the encoder and decoder. The motion codebook has 512 vectors of $D (= 256)$ dimensions, and the attention widths are $M = 100$ and $M = 10$ for the encoder and decoder, respectively.

Differences between the subjects can be visualized by comparing their motion code structures, which are shown in Fig. 6. Here, half of the motion

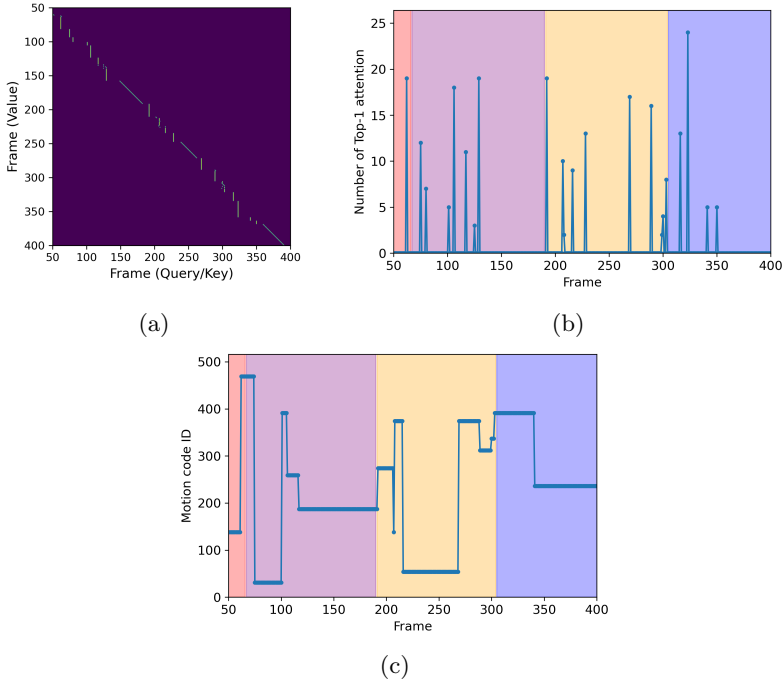


Fig. 4 (a) Top-1 frames for each value vector, (b) Number of times counted as top-1 attention frames, which is used to extract keyframes, (c) Motion code transitions assigned to the keyframes

codes are shared by both subjects, and the others are only used by one of the subjects, which indicates that the motion codes can express both the similarities and uniqueness of the subjects.

4.1 Evaluating the latent space by linear probing of multiple tasks

For quantitative evaluation of the latent space generated by the proposed method, the task of recognizing annotated labels was tested by using the motion codes as the input. The purpose was to evaluate whether the generated motion codes, which are trained by reconstructing the output vectors, contain useful information. Since fine-tuning the trained network to a specific task is not an appropriate method by which to evaluate the usefulness of motion codes, linear probing with a simple linear layer, in which the backbone network to generate latent space is fixed, was applied.

Since the motion codes have sufficient structure to allow them to reconstruct human motion, the generated motion codes are expected to be applicable to multiple tasks without optimization to specific tasks. In the present study, two tasks, action segmentation and skill classification, are tested with the JIGSAWS dataset. The former is a task that assigns action labels for each frame,

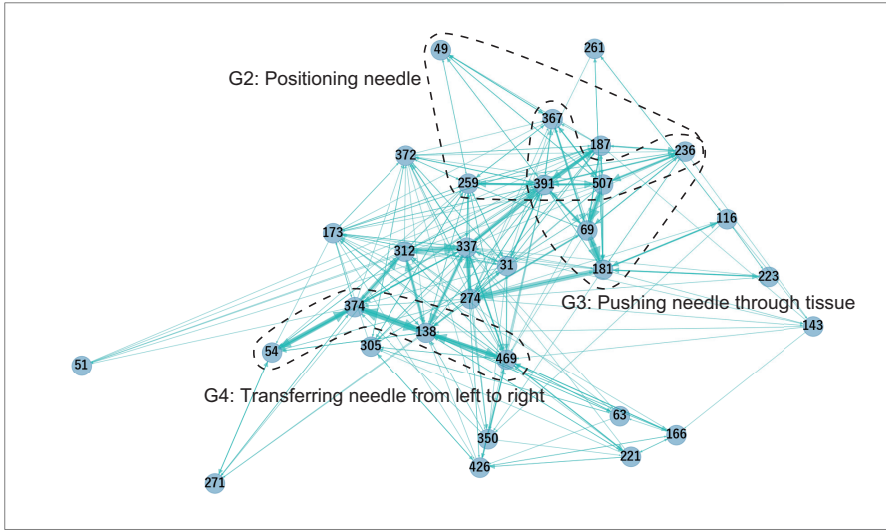


Fig. 5 Graph of keyframe motion codes is constructed by the transition. The numbers indicate the IDs of motion codes. The relationship between the annotation labels is visualized in the graph

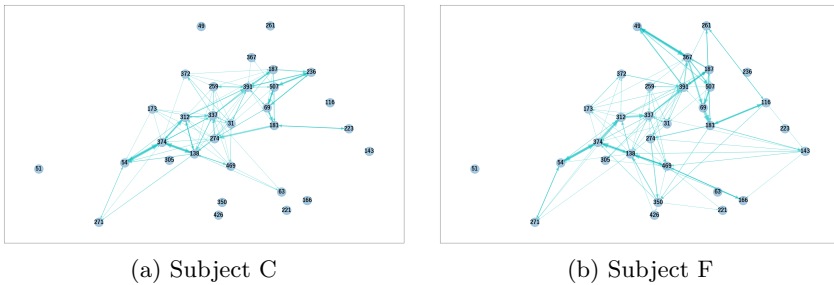


Fig. 6 Keyframe motion code graphs for two subjects for different sets of motion codes

and the latter involves classifying each sequence to one of the skill levels. The head blocks are trained for these tasks by a single linear layer.

As the baseline methods, the network for skill classification by Ismail et al. [42] and temporal convolutional networks (TCNs) [43] for action segmentation are compared. As shown in Fig. 7, the backbone and head blocks for the designed tasks are trained end-to-end for each method, and the head for the other task is trained as linear probing. Except for the input dimension, the head block architectures are the same for the three methods. The input vector of the linear layers is the quantized feature vector of the motion codes. The linear layer of action segmentation uses a part of the sequence as the input and is implemented as a 1D convolution. The 1D convolution of the head for action segmentation uses 500 frames around each frame.

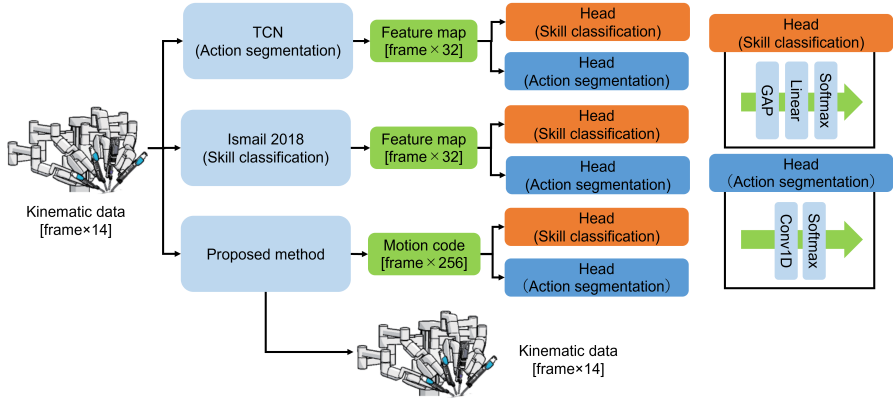


Fig. 7 Evaluation of motion codes by linear probing with JIGSAWS kinematic inputs

Tables 1 and 2 show the quantitative results of action segmentation and skill classification, respectively. The accuracy is the percentage of correctly labeled frames, and the edit score is the segmental edit distance [43] to measure the correctness of the temporal ordering of actions. The micro average accuracy and the macro average recall [44] are computed as the average of total correct predictions across all classes and the mean of true positive rates for each class, respectively. The compared methods that are optimized to one of the two tasks show good results for the optimized tasks, but the results for the other task by linear probing are degraded. Although the proposed method is not optimized for each task, the results are comparable to the method optimized for each task. This proves that the motion codes extract effective information to understand the temporal structure of motion and to explain the static characteristics between motions.

Table 1 Results of action segmentation for JIGSAWS kinematic inputs

	Accuracy	Edit score
Ismail 2018[42]	64.9	55.9
TCN[43]	80.3	85.6
MotionCode (Proposed)	82.6	65.7

Table 2 Results of skill classification for JIGSAWS kinematic inputs

	Micro average accuracy	Macro average recall
Ismail 2018[42]	99.4	99.6
TCN[43]	59.0	46.7
MotionCode (Proposed)	94.9	94.9

4.2 Evaluation with video/3D skeleton inputs

4.2.1 Extracting motion codes from video

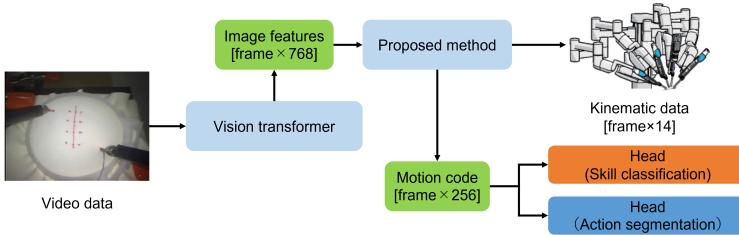


Fig. 8 Evaluation of motion codes by linear probing with JIGSAWS video inputs

The next experiment is extracting motion codes from the video in the JIGSAWS dataset, which means that the output modality is different from that of the input. In this experiment, each frame in a video is encoded as a feature frame by frame using an image encoding block, and the feature is used as the input of the proposed encoder-decoder model, as shown in Fig. 8. The image encoding is implemented by Vision transformer [45], and the parameters are fine-tuned to predict the kinematic data of each frame. The dimension of the feature vector used as input is 768. Since no implementation is available to test the tasks of action segmentation and skill classification from video, the proposed method is compared with the methods tested under the same condition. The results obtained by MsM-CRF [44] and 3D ConvNet [46] are shown for comparison in Tables 3 and 4 for action segmentation and skill classification, respectively. Although the recognition by the proposed method is linear probing without fine-tuning, the results of the proposed method are comparable with those of the methods that are optimized for the respective tasks.

Table 3 Results of action segmentation for JIGSAWS video inputs

	Micro average accuracy	Macro average recall
MsM-CRF [44]	84.4	71.8
MotionCode (Proposed)	82.5	70.9

Table 4 Results of skill classification for JIGSAWS video inputs

	Micro average accuracy	Macro average recall
3D ConvNet [46]	100	100
MotionCode (Proposed)	94.9	96.5

4.2.2 Extracting motion codes from a 3D skeleton

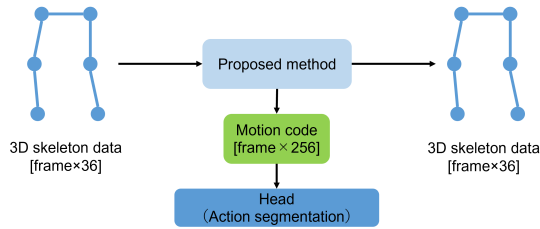


Fig. 9 Evaluation of motion codes by linear probing with 3D skeleton inputs

The next experiment is extracting the motion codes from a 3D skeleton dataset (HuGaDB) [47], as shown in Fig. 9. The dataset contains the motions of the lower half of the body, such as walking, taking stairs up or down, and sitting down, with segmentation and annotation. The input skeleton consists of six joints with a three-axis accelerometer and three-axis gyroscope data at each joint. The motions are captured at 60Hz for 18 subjects, and their lengths are 300 frames to 12,000 frames. The split of training and test sequences is the same as the setting in [48]. The results are evaluated by accuracy and F1@50. The former is sample-wise accuracy, as described above, and the latter is the F1-score of classifying segments by 50% intersection over union (IoU) overlap with respect to the corresponding expert annotation [27]. Table 5 shows the results compared with the methods tested in [48]. The accuracy of the proposed method is comparable to those of the other methods that optimized for the segmentation task, although the F1@50 score is lower than those of the others, which is the case because no device is provided to avoid over-segmentation in linear probing, as is the edit score in Table 1.

Table 5 Results of action segmentation for the 3D skeleton dataset (HuGaDB)

	Accuracy	F1@50
Bi-LSTM	86.1	81.5
TCN	88.3	56.8
ST-GCN	88.7	67.7
MS-TCN	86.8	89.9
MS-GCN	90.4	93.0
MotionCode (Proposed)	87.5	58.5

4.3 Ablation study

4.3.1 Generating motion codes without restriction

Restricting motion codes in the training introduced in Section 3.3.3 is expected to encourage motion code sharing. Fig. 10 shows a comparison of the results

of training with and without restriction. In the restricted case, most of the motion codes used by subjects C and F are shared, which indicates that the motions are translatable to each other between the subjects. On the other hand, in the non-restricted case, most of the motion codes are not shared between subjects C and F. The reconstruction loss decreases more easily by using different motion codes than by sharing motion codes, however, using split codes is not desirable for translatability. The result shows the need for restrictions to share motion codes between subjects.

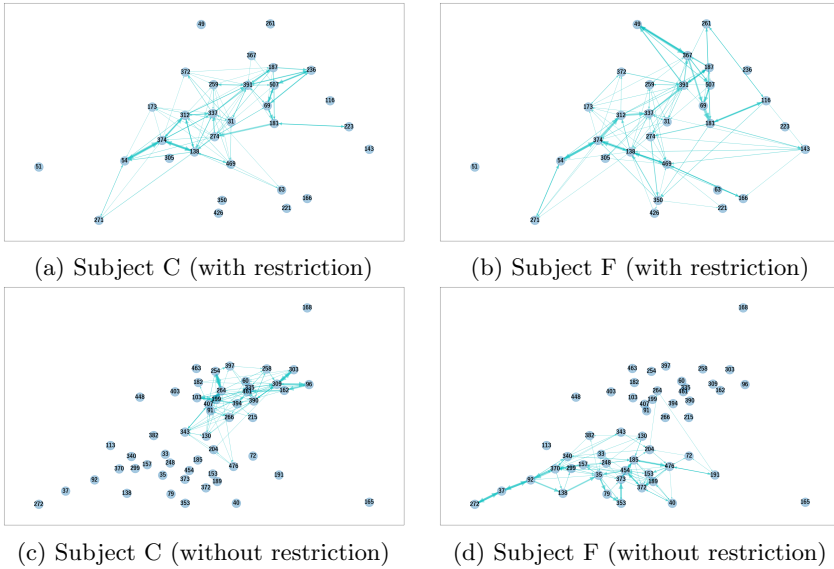


Fig. 10 Motion code graphs for the results trained with / without restricting motion codes

4.3.2 Effect of the attention width of the decoder

Attention width M of the decoder attention layers defines how many preceding frames are referred to generate motion from motion codes. The number of reference frames is expected to affect the frame range of high attention weight to a keyframe. In this experiment, how the sequence of extracted motion codes changes is tested if the reference frames are wide. The attention width M is changed to 100 while $M = 10$ in Fig. 4. Fig. 11 shows the entire sequence of keyframe motion codes with (a) $M = 10$ and with (b) $M = 100$. Since the total attention widths of six attention layers are 60 and 600, respectively, the attention is concentrated on sparse keyframes and the number of keyframes is reduced in the latter case. Since the boundaries between different motion codes are still close to those of the annotated labels, the motion codes have a relationship to the understanding of motion by humans. Tables 6 and 7 shows the results of action segmentation and skill classification by attention width of

the decoder, respectively. Since the performance of action segmentation with $M = 100$ is similar to the case with $M = 10$, the motions can be recognized in the case of sparse keyframes. On the other hand, the result of skill classification is degraded with $M = 100$ from the case with $M = 10$. The reason is considered to be because, as shown in Fig. 12, in the case of $M = 100$, most motion codes are shared by subjects compared to the case of $M = 10$. Consequently, the granularity of motion codes can be controlled by the parameter of the attention width, but the side effect of sharing motion codes is an issue to be investigated in a future study.

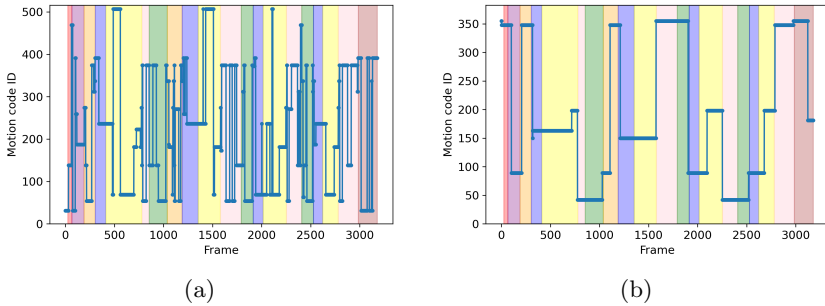


Fig. 11 Transition of keyframe motion codes with (a) $M = 10$ and (b) $M = 100$

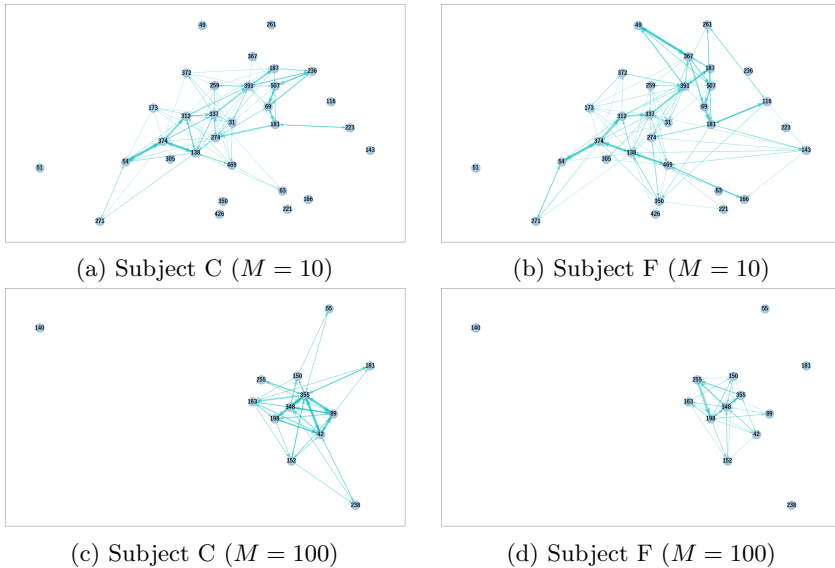


Fig. 12 Motion code graphs with $M = 10$ and $M = 100$

Table 6 Results of action segmentation for JIGSAWS kinematic inputs based on the attention width of the decoder

Attention width M	Accuracy	Edit score
10	82.6	65.7
100	82.7	64.3

Table 7 Results of skill classification for JIGSAWS kinematic inputs based on the attention width of the decoder

Attention width M	Micro average accuracy	Macro average recall
10	94.9	94.9
100	88.5	88.2

5 Conclusion

In the present paper, we proposed an encoder-decoder model that extracts frame-wise motion codes as discrete components in order to provide intermediate representations of human motions. The motion codes are extracted in a self-supervised manner without using any manual annotations. We found that generating a discrete representation contributes to extracting sparse keyframes and visualizing the relationship between the components. We then evaluated the effectiveness of the motion codes by applying them to multiple recognition tasks. Since the motion codes extracted by the proposed method yield results comparable to those that have features optimized by supervised learning, the results of the present study show that the motion codes contain sufficient information to effectively understand human motions.

One of the issues is optimizing the granularity of the motion codes for various tasks. When the attention width is narrow, the granularity is smaller than that of annotation labels, which makes it difficult to find one-to-one correspondence with a user-defined label. Furthermore, since various levels of granularity can be considered when attempting to explain human behavior, one of our future areas of study will be to generate a hierarchical structure of motion codes. More specifically, since structures can be extracted in a self-supervised manner from the dataset used, the goal will be to construct a hierarchical motion code structure without the need for hand-crafted level explanations of human behavior. In addition, since the advantages of the sparse and discrete features make them easily specified by users, another direction of future study will be to use motion codes to generate new motions that may be difficult to explain by user-defined labels. Such motions can be expected to be useful for robotics and computer graphics applications.

Acknowledgments. This work was supported by JSPS JP22H00545, JP22H05002 and NEDO JPNP20006 (New Energy and Industrial Technology Development Organization) in Japan.

Declarations

Conflict of interest The authors declare that they have no conflict of interest.

Appendix A Keyframe motion code graph

In our experiments, we tested three types of input data. Figs. 13, 14, 15 show the keyframe motion code graphs of all individual subjects for JHU-ISI gesture and skill assessment working set (JIGSAWS) kinematic inputs, JIGSAWS video inputs and 3D skeleton inputs (HuGaDB), respectively. As described in the main manuscript, there are differences in the codes used between the subjects.

Online Resource 1 (ESM.1.mp4) shows the synchronized visualization of the input video and the keyframe motion codes for the two sequences of the JIGSAWS kinematic inputs, `Suturing_C001` of Subject C and `Suturing_F001` of Subject F. One of the clear differences is the IDs of motion codes used for the annotation, “Pushing needle through tissue”. The IDs, 49 and 236, are used by one of the two subjects, but not by the other subject. The difference occurs repeatedly, and the reason for the difference is considered to be caused by the difference of the gripper pose. Since we do not have expert knowledge of robotic surgery, we cannot tell whether it comes from the skill or habit of a subject, but the similarities and uniqueness are visualized without the knowledge. Online Resource 2 (ESM.2.mp4) shows a comparison of changing the decoder attention width. If the attention width is large ($M = 100$), the motion is represented by a smaller number of keyframe motion codes than in the case of small attention width ($M = 10$). Since each segment becomes long, the granularity of the motion codes is coarse. The control of the granularity is one of our future areas of study. Online Resource 3 (ESM.3.mp4) shows the synchronized visualization of the input video and the keyframe motion codes for the two sequences of the JIGSAWS video inputs, `Suturing_C001` of Subject C and `Suturing_F001` of Subject F. The difference between subjects C and F can be also observed, even if the input is changed to videos. For example, the codes used in the annotation, “Pushing needle through tissue”, are different.

Appendix B Action segmentation

Fig. 16 gives a visual overview of the action segmentation results for JIGSAWS kinematic input. The left-hand column in the figure shows the results of the test split with the highest accuracy in quantitative evaluation, whereas the right-hand column shows the results of the test split of the worst case. The action segmentation is accomplished with high quality for most of the sequences. The sequences `Suturing_H001` and `Suturing_I001` are examples of the worst case. The reason for their difference from the ground truth is considered to be due to insufficient data because “Loosening more suture” appears in only one sequence in this training split (and appears in only three sequences in the total

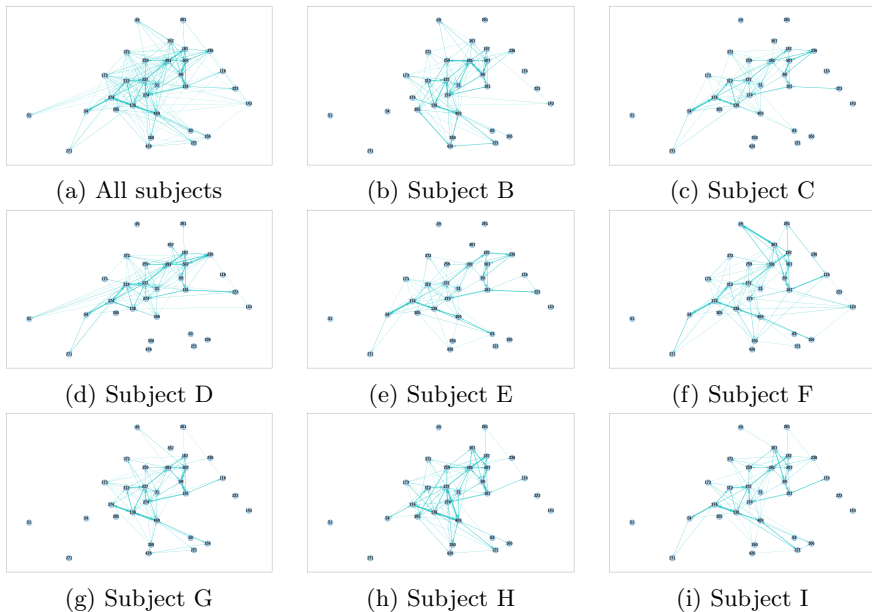


Fig. 13 Keyframe motion code graphs for all subjects. The kinematic data are used as input

dataset). In addition, since the subjects repeatedly try and fail the operation in the sequences of `Suturing_B001` and `Suturing_G001`, over-segmentation occurs in these cases and results in low edit scores.

Fig. 17 gives a visual overview of the action segmentation results for JIGSAWS video input. The left-hand column in the figure shows the results for the test split with the highest accuracy in quantitative evaluation, whereas the right-hand column shows the results for the test split of the worst case. The segmentation quality of the video input is slightly more accurate than the result for the kinematic input. The results of video input are believed to be more accurate because the input and output are close to the condition of annotation, which is given by watching videos. The difference from the ground truth is considered to be due to the same reason in the case of kinematic input, insufficient training examples and over-segmentation of repeated trials in an operation.

Fig. 18 gives a visual overview of the action segmentation results for HuGaDB. The sequences in the figure are from the test dataset, excluding duplicate combinations of actions. The action segmentation is accomplished with high accuracy for most of the sequences. Although the proposed method is based on reconstructing acceleration and angular velocity, these factors do not have significant differences between certain annotations, for example, between “Walking” and “Going up/down” and between “Standing” and “Up/down by elevator”, which are considered to be the reason for the incorrect classification found in `02_00`, `03_05`, and `04_13`.

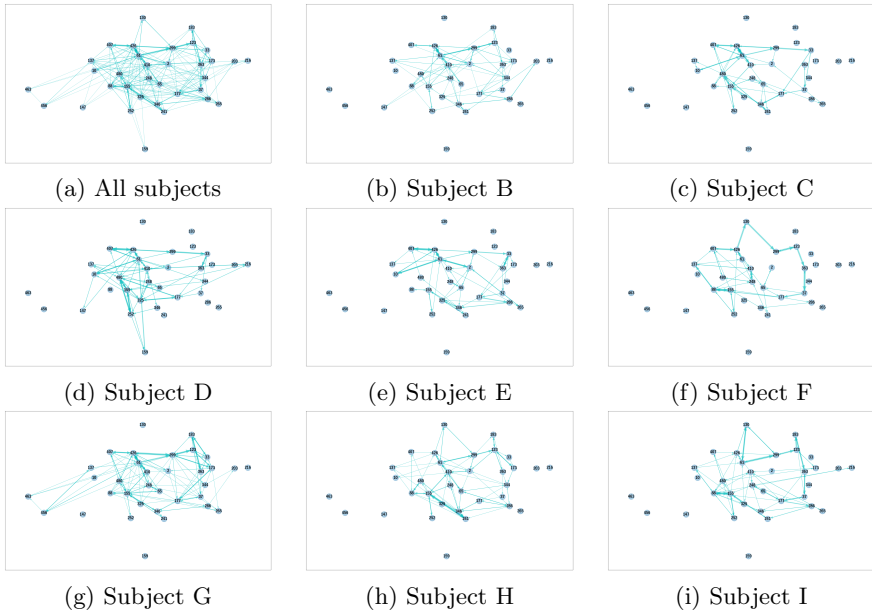


Fig. 14 Keyframe motion code graphs for all subjects. The video data are used as input

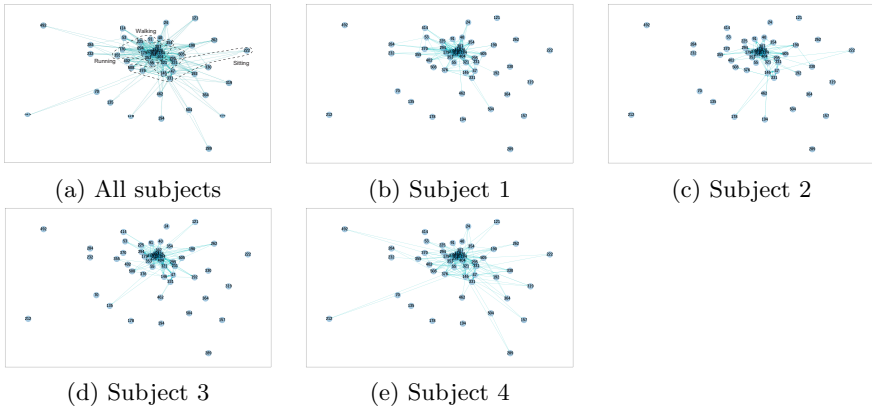


Fig. 15 Keyframe motion code graphs for all subjects in HuGaDB. The dotted lines enclose the motion codes used for Walking, Running, and Sitting

References

- [1] Su K, Liu X, Shlizerman E (2020) Predict & cluster: Unsupervised skeleton based action recognition. In: Proceedings of the IEEE/CVF Conference on Computer Vision and Pattern Recognition, pp 9631–9640, <https://doi.org/10.1109/CVPR42600.2020.00965>
- [2] Lin L, Song S, Yang W, et al (2020) Ms2l: Multi-task self-supervised learning for skeleton based action recognition. In: Proceedings of the 28th

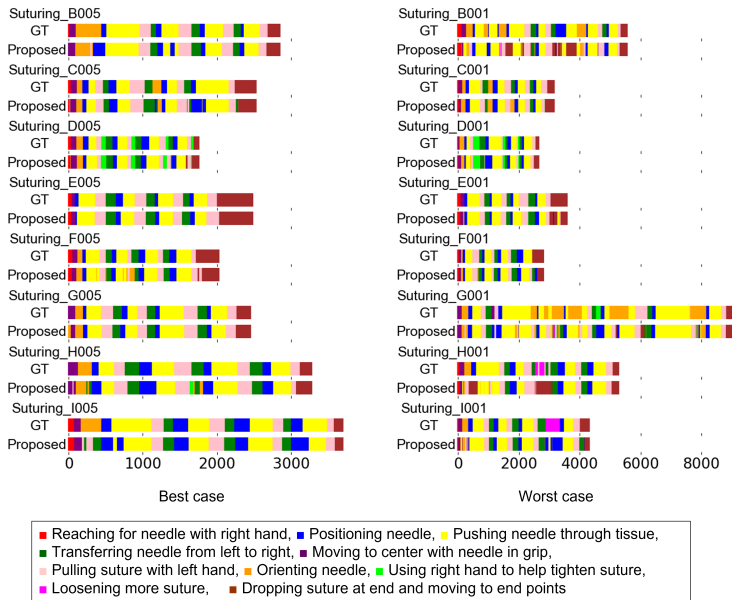


Fig. 16 Action segmentation results of JIGSAWS kinematic input

ACM International Conference on Multimedia, pp 2490–2498, <https://doi.org/10.1145/3394171.3413548>

- [3] Thoker FM, Doughty H, Snoek CG (2021) Skeleton-contrastive 3d action representation learning. In: Proceedings of the 29th ACM International Conference on Multimedia, pp 1655–1663, <https://doi.org/10.1145/3474085.3475307>
- [4] Girdhar R, Ramanan D, Gupta A, et al (2017) Actionvlad: Learning spatio-temporal aggregation for action classification. In: Proceedings of the IEEE Conference on Computer Vision and Pattern Recognition, pp 971–980, <https://doi.org/10.1109/CVPR.2017.337>
- [5] Wang X, Zhang S, Qing Z, et al (2021) Oadtr: Online action detection with transformers. arXiv preprint arXiv:210611149 <https://doi.org/10.1109/ICCV48922.2021.00747>
- [6] Sigurdsson GA, Divvala S, Farhadi A, et al (2017) Asynchronous temporal fields for action recognition. In: Proceedings of the IEEE conference on Computer Vision and Pattern Recognition, pp 585–594, <https://doi.org/10.1109/CVPR.2017.599>
- [7] Shi L, Zhang Y, Cheng J, et al (2021) Adasgn: Adapting joint number and model size for efficient skeleton-based action recognition. arXiv preprint

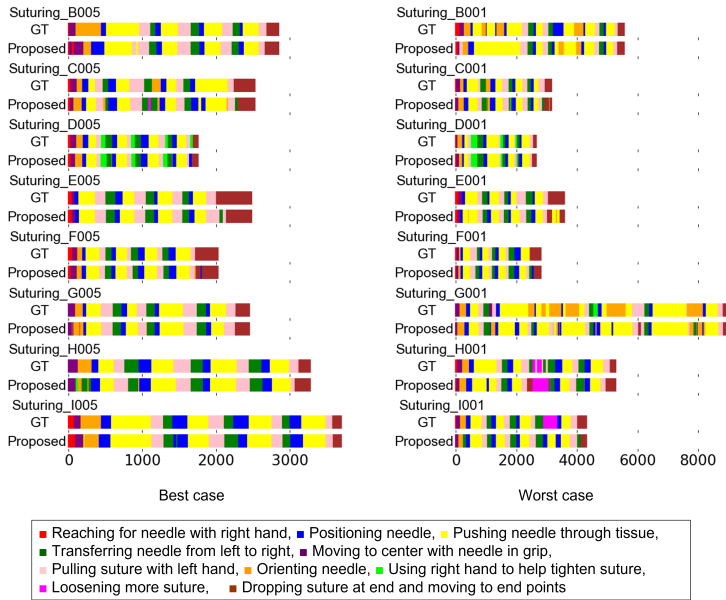


Fig. 17 Action segmentation results of JIGSAWS video input

arXiv:210311770

- [8] Duan H, Zhao Y, Chen K, et al (2021) Revisiting skeleton-based action recognition. arXiv preprint arXiv:210413586 <https://doi.org/10.1109/CVPR52688.2022.00298>
- [9] Yan S, Xiong Y, Lin D (2018) Spatial temporal graph convolutional networks for skeleton-based action recognition. In: Thirty-second AAAI conference on artificial intelligence
- [10] Takano W, Nakamura Y (2008) Integrating whole body motion primitives and natural language for humanoid robots. In: Humanoids 2008-8th IEEE-RAS International Conference on Humanoid Robots, IEEE, pp 708–713, <https://doi.org/10.1109/ICHR.2008.4755976>
- [11] Takano W, Nakamura Y (2015) Statistical mutual conversion between whole body motion primitives and linguistic sentences for human motions. The International Journal of Robotics Research 34(10):1314–1328. <https://doi.org/10.1177/0278364915587923>
- [12] Plappert M, Mandery C, Asfour T (2018) Learning a bidirectional mapping between human whole-body motion and natural language using deep recurrent neural networks. Robotics and Autonomous Systems 109:13–26. <https://doi.org/10.1016/j.robot.2018.07.006>

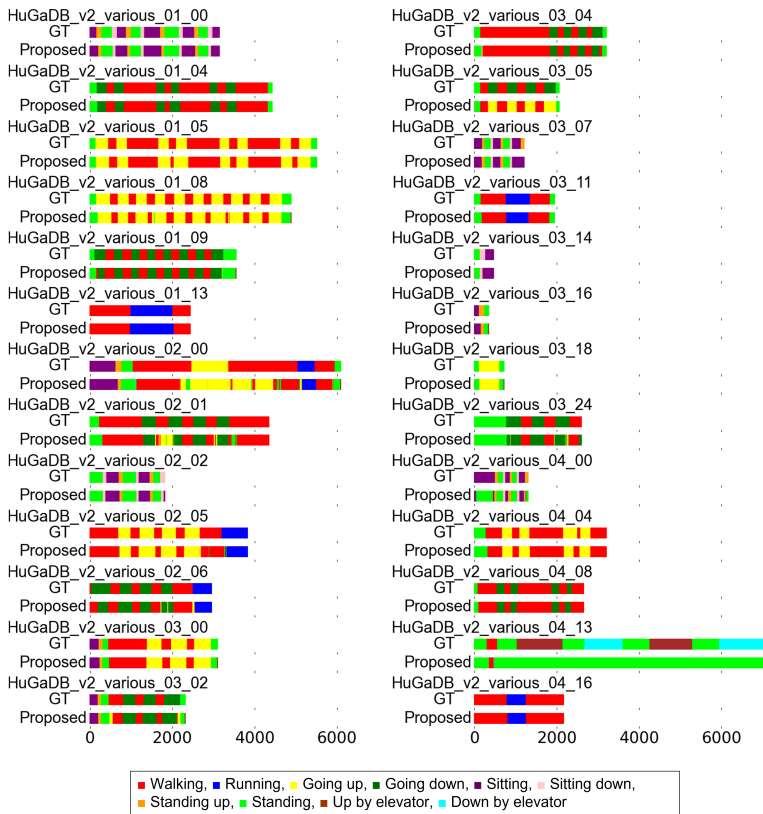


Fig. 18 Action segmentation results of HuGaDB

- [13] Ahn H, Ha T, Choi Y, et al (2018) Text2action: Generative adversarial synthesis from language to action. In: 2018 IEEE International Conference on Robotics and Automation (ICRA), IEEE, pp 5915–5920, <https://doi.org/10.1109/ICRA.2018.8460608>
- [14] Yamada T, Matsunaga H, Ogata T (2018) Paired recurrent autoencoders for bidirectional translation between robot actions and linguistic descriptions. *IEEE Robotics and Automation Letters* 3(4):3441–3448. <https://doi.org/10.1109/LRA.2018.2852838>
- [15] Ahuja C, Morency LP (2019) Language2pose: Natural language grounded pose forecasting. In: 2019 International Conference on 3D Vision (3DV), IEEE, pp 719–728, <https://doi.org/10.1109/3DV.2019.00084>
- [16] Misra I, Zitnick CL, Hebert M (2016) Shuffle and learn: unsupervised learning using temporal order verification. In: European Conference on Computer Vision, Springer, pp 527–544, <https://doi.org/10.1007/>

[978-3-319-46448-0_32](#)

- [17] Su Y, Lin G, Wu Q (2021) Self-supervised 3d skeleton action representation learning with motion consistency and continuity. In: Proceedings of the IEEE/CVF International Conference on Computer Vision, pp 13,328–13,338, <https://doi.org/10.1109/ICCV48922.2021.01308>
- [18] Farha YA, Gall J (2019) Ms-tcn: Multi-stage temporal convolutional network for action segmentation. In: Proceedings of the IEEE/CVF Conference on Computer Vision and Pattern Recognition, pp 3575–3584, <https://doi.org/10.1109/CVPR.2019.00369>
- [19] Huang Y, Sugano Y, Sato Y (2020) Improving action segmentation via graph-based temporal reasoning. In: Proceedings of the IEEE/CVF Conference on Computer Vision and Pattern Recognition, pp 14,024–14,034, <https://doi.org/10.1109/CVPR42600.2020.01404>
- [20] Chen MH, Li B, Bao Y, et al (2020) Action segmentation with joint self-supervised temporal domain adaptation. In: Proceedings of the IEEE/CVF Conference on Computer Vision and Pattern Recognition, pp 9454–9463, <https://doi.org/10.1109/CVPR42600.2020.00947>
- [21] Li J, Todorovic S (2021) Action shuffle alternating learning for unsupervised action segmentation. In: Proceedings of the IEEE/CVF Conference on Computer Vision and Pattern Recognition, pp 12,628–12,636
- [22] Del Pero L, Ricco S, Sukthankar R, et al (2015) Articulated motion discovery using pairs of trajectories. In: Proceedings of the IEEE conference on computer vision and pattern recognition, pp 2151–2160, <https://doi.org/10.1109/CVPR.2015.7298827>
- [23] Sarfraz S, Murray N, Sharma V, et al (2021) Temporally-weighted hierarchical clustering for unsupervised action segmentation. In: Proceedings of the IEEE/CVF Conference on Computer Vision and Pattern Recognition, pp 11,225–11,234
- [24] Dwibedi D, Aytaar Y, Tompson J, et al (2019) Temporal cycle-consistency learning. In: Proceedings of the IEEE/CVF Conference on Computer Vision and Pattern Recognition, pp 1801–1810, <https://doi.org/10.1109/CVPR.2019.00190>
- [25] Lan T, Zhu Y, Zamir AR, et al (2015) Action recognition by hierarchical mid-level action elements. In: Proceedings of the IEEE international conference on computer vision, pp 4552–4560, <https://doi.org/10.1109/ICCV.2015.517>

- [26] Pirsiavash H, Ramanan D (2014) Parsing videos of actions with segmental grammars. In: Proceedings of the IEEE conference on computer vision and pattern recognition, pp 612–619, <https://doi.org/10.1109/CVPR.2014.85>
- [27] Lea C, Flynn MD, Vidal R, et al (2017) Temporal convolutional networks for action segmentation and detection. In: proceedings of the IEEE Conference on Computer Vision and Pattern Recognition, pp 156–165, <https://doi.org/10.1109/CVPR.2017.113>
- [28] Lea C, Reiter A, Vidal R, et al (2016) Segmental spatiotemporal cnns for fine-grained action segmentation. In: European Conference on Computer Vision, Springer, pp 36–52, https://doi.org/10.1007/978-3-319-46487-9_3
- [29] Richard A, Kuehne H, Gall J (2017) Weakly supervised action learning with rnn based fine-to-coarse modeling. In: Proceedings of the IEEE conference on Computer Vision and Pattern Recognition, pp 754–763, <https://doi.org/10.1109/CVPR.2017.140>
- [30] Sener F, Yao A (2018) Unsupervised learning and segmentation of complex activities from video. In: Proceedings of the IEEE Conference on Computer Vision and Pattern Recognition, pp 8368–8376, <https://doi.org/10.1109/CVPR.2018.00873>
- [31] Jain A, Zamir AR, Savarese S, et al (2016) Structural-rnn: Deep learning on spatio-temporal graphs. In: Proceedings of the IEEE conference on computer vision and pattern recognition, pp 5308–5317, <https://doi.org/10.1109/CVPR.2016.573>
- [32] Guo C, Zuo X, Wang S, et al (2020) Action2motion: Conditioned generation of 3d human motions. In: Proceedings of the 28th ACM International Conference on Multimedia, pp 2021–2029, <https://doi.org/10.1145/3394171.3413635>
- [33] Ghosh P, Song J, Aksan E, et al (2017) Learning human motion models for long-term predictions. In: 2017 International Conference on 3D Vision (3DV), IEEE, pp 458–466, <https://doi.org/10.1109/3DV.2017.00059>
- [34] Butepage J, Black MJ, Kragic D, et al (2017) Deep representation learning for human motion prediction and classification. In: Proceedings of the IEEE conference on computer vision and pattern recognition, pp 6158–6166, <https://doi.org/10.1109/CVPR.2017.173>
- [35] van den Oord A, Vinyals O, Kavukcuoglu K (2017) Neural discrete representation learning. CoRR abs/1711.00937. URL <http://arxiv.org/abs/1711.00937>, <https://arxiv.org/abs/arXiv:1711.00937>

- [36] Ramesh A, Pavlov M, Goh G, et al (2021) Zero-shot text-to-image generation. CoRR abs/2102.12092. URL <https://arxiv.org/abs/2102.12092>, <https://arxiv.org/abs/arXiv:2102.12092>
- [37] Vaswani A, Shazeer N, Parmar N, et al (2017) Attention is all you need. In: Advances in neural information processing systems, pp 5998–6008
- [38] Kingma DP, Welling M (2013) Auto-encoding variational bayes. arXiv preprint arXiv:13126114
- [39] Gao Y, Vedula SS, Reiley CE, et al (2014) Jhu-isi gesture and skill assessment working set (jigsaws): A surgical activity dataset for human motion modeling. In: MICCAI workshop: M2cai
- [40] Fruchterman TM, Reingold EM (1991) Graph drawing by force-directed placement. *Software: Practice and experience* 21(11):1129–1164. <https://doi.org/10.1002/spe.4380211102>
- [41] Hagberg AA, Schult DA, Swart PJ (2008) Exploring network structure, dynamics, and function using networkx. In: Varoquaux G, Vaught T, Millman J (eds) Proceedings of the 7th Python in Science Conference, Pasadena, CA USA, pp 11 – 15
- [42] Ismail Fawaz H, Forestier G, Weber J, et al (2018) Evaluating surgical skills from kinematic data using convolutional neural networks. In: International Conference on Medical Image Computing and Computer-Assisted Intervention, Springer, pp 214–221, https://doi.org/10.1007/978-3-030-00937-3_25
- [43] Lea C, Vidal R, Reiter A, et al (2016) Temporal convolutional networks: A unified approach to action segmentation. In: European conference on computer vision, Springer, pp 47–54, https://doi.org/10.1007/978-3-319-49409-8_7
- [44] Ahmidi N, Tao L, Sefati S, et al (2017) A dataset and benchmarks for segmentation and recognition of gestures in robotic surgery. *IEEE Transactions on Biomedical Engineering* 64(9):2025–2041. <https://doi.org/10.1109/TBME.2016.2647680>
- [45] Dosovitskiy A, Beyer L, Kolesnikov A, et al (2020) An image is worth 16x16 words: Transformers for image recognition at scale. arXiv preprint arXiv:201011929
- [46] Funke I, Mees ST, Weitz J, et al (2019) Video-based surgical skill assessment using 3d convolutional neural networks. *International journal of computer assisted radiology and surgery* 14(7):1217–1225. <https://doi.org/10.1007/s11548-019-01995-1>

- [47] Chereshev R, Kertész-Farkas A (2017) Hugadb: Human gait database for activity recognition from wearable inertial sensor networks. In: International Conference on Analysis of Images, Social Networks and Texts, Springer, pp 131–141, https://doi.org/10.1007/978-3-319-73013-4_12
- [48] Filtjens B, Vanrumste B, Slaets P (2022) Skeleton-based action segmentation with multi-stage spatial-temporal graph convolutional neural networks. arXiv preprint arXiv:220201727 <https://doi.org/10.1109/TETC.2022.3230912>